

Electronic structure of defects and impurities in a-Si

This article has been downloaded from IOPscience. Please scroll down to see the full text article.

1990 J. Phys.: Condens. Matter 2 6519

(<http://iopscience.iop.org/0953-8984/2/31/004>)

View [the table of contents for this issue](#), or go to the [journal homepage](#) for more

Download details:

IP Address: 171.66.16.103

The article was downloaded on 11/05/2010 at 06:02

Please note that [terms and conditions apply](#).

Electronic structure of defects and impurities in a-Si

Bal K Agrawal, Savitri Agrawal, P S Yadav and J S Negi
Physics Department, Allahabad University, Allahabad 211002, India

Received 24 July 1989, in final form 28 February 1990

Abstract. A theoretical study of the electronic structure of shallow and deep electron states caused by quantitative disorder, relaxed defects and impurity atoms in amorphous silicon has been made by using the cluster Bethe lattice method incorporating an LCAO (linear combination of atomic orbitals) basis set. Although localised states in the neighbourhood of the band edges of the fundamental gap arise from both the Si–Si bond length elongation and bond angle disorder, the effects of bond angle variance are more dominant. Similarly for the relaxed dangling bond, quite a small shift in the location of the state in the gap occurs by Si–Si bond length changes but significant shifts appear as a result of the variation in Si–Si bond angles. Thus, the state energy changes from 0.49 to 1.55 eV for a variation in the bond angle by -10% to $+10\%$. Localised/resonance states possessing A_1 and/or T_2 symmetry appear throughout the band gap for all the interstitial atoms belonging to groups II to VI of the periodic table and for most of the substitutional atoms. Gap states are not seen for the small-sized substitutional atoms like Be and B. The electronegativity of an impurity does not seem to play any role in determining the location of the state in the fundamental gap. The present results are in good qualitative and semi-quantitative agreement with the experimental and self-consistent pseudopotential calculation results wherever they are available for either crystalline or amorphous silicon.

1. Introduction

Great interest has been shown in the literature towards the study of the role of defects and imperfections in generating new electronic energy states, especially states in the fundamental electronic energy gap in amorphous semiconductors. This interest stems from the fact that these gap states, which very often provide effective non-radiative recombination centres, play an essential role in determining many structural, electronic and transport properties of these materials necessary for their future applications in electronic, opto-electronic and other types of devices.

States in the gap may originate from structural defects such as bond elongation, bond and dihedral angle variations, vacancies and divacancies, etc., and their complexes in tetrahedral semiconductors. In general, the localised states appearing near the fundamental gap edges, often referred to as tail states, arise mainly from structural disorder such as the variations in bond lengths, interatomic bond angles and the various atomic energies. The so-called shallow levels in the gap originate usually from dopant atoms. On the other hand, levels lying close to the gap centre in the fundamental gap, called deep levels, are mostly produced by dangling bonds, vacancies and their complexes with themselves or with impurity atoms, or by foreign atoms at substitutional or interstitial positions.

The role of group III and V elements as dopants at substitutional sites does not need to be emphasised. In crystalline Si (c-Si) they are known to produce shallow states having quite extended wavefunctions. While heavy doping in c-Si causes a degenerate semiconductor, in hydrogenated a-Si, on the other hand, the Fermi level (E_F) can only be moved to within 0.1–0.15 eV of a band edge. The question why doping does not push the Fermi level into the impurity band in a-Si has been discussed earlier by Street (1982) and Robertson (1983). E_F does not seem to lie in the dopant band. This behaviour of a-Si:H may be partially explained if the common dopants produce a deep gap state in the large band gap of 1.8 eV in a-Si:H. The electronic structure of group III and V elements in a-Si thus needs to be investigated. Interest in the chalcogens in silicon has been largely for technological reasons. For example, the atoms Se and Te are candidates for use in infrared detectors, while S is the main contaminant in solar-grade Si produced by alumino-thermic reduction from metallurgical Si. These chalcogenide atoms produce deep levels, as shown by large shifts under applied hydrostatic pressure.

For crystalline phases, first-principles methods like density-functional theory (Scheffler *et al* 1984, Baraff and Schluter 1984, Bar-Yam and Joannopoulos 1984) have been developed to the point where electron and exchange correlations are treated either exactly or approximately in order to make the equations tractable. However, accurate calculations are possible at present only for simple point defects and for periodic structures with small unit cells. Defect complexes of more than three atoms and low symmetry surfaces or steps have not yet been investigated by such first-principles calculations. For amorphous systems, on the other hand, the calculation of the electronic band structure from first principles is quite difficult because of the absence of lattice periodicity seen in the crystalline phase. Bloch's theorem is no longer applicable and the concept of k as a good quantum number is not valid. One has, thus, to develop direct-space methods. However, they may be numerically much less involved than k -space models and allow one to bring out the essential physics of these systems.

One such model is based on the pseudo-lattice, or cluster Bethe lattice. The amorphous network is simulated by a Cayley tree, which is an infinite aperiodic open structure devoid of any rings. Although, the lattice is unphysical, its treatment does not involve any approximation. The thermodynamic equalities are thus maintained. Very often, in the diagrammatic expansion of real lattices, the first (and often only) set of diagrams that can be summed are tree diagrams that correspond to a Bethe lattice. In the cluster Bethe lattice method one considers a finite cluster of atoms containing defects or impurities and couples the surface atoms of the cluster to the Bethe lattice, thus avoiding the extra unwarranted features that arise from the surface atoms of the cluster. Previous results obtained for the various complex amorphous systems have been very encouraging. Fedders and Carlsson (1987, 1988, 1989) have very recently discussed the controversy between the so-called floating and dangling bonds using this method.

We are presently involved in a study of complexes formed from simple defects that have been identified in or speculated to be present in the various types of experimental measurements and have been shown to control device properties and their applications. The present paper is the first report of a series and is concerned with an investigation of simple point defects, various complexes of which are to be reported later. We have used a cluster Bethe lattice method (CBLM) involving a linear combination of atomic orbitals (LCAO) in a tight-binding approximation.

The details of the calculations are contained in section 2, while the electronic structure of the structural defects such as the relaxed dangling bonds are contained in section 3. Section 4 contains the results for the gap states incurred by the substitutional and interstitial impurity atoms and ions. Section 5 includes the main conclusions.

Table 1. Parameters used in calculation of defects in a-Si (eV).

Atom/orbital	E_s	E_p			E_{s^*}	
Si	-3.95	2.3			7.25	
Interaction	Bond	U	V	X	T	H
First neighbour	Si-Si	-1.94	1.73	1.01	0.66	0.88

2. Calculations

We have used the standard cluster Bethe lattice method (CBLM) and a basis set consisting of five localised orbitals designated as s , p_x , p_y , p_z , s^* (Vogl *et al* 1983). The choice of the Hamiltonian matrix elements is difficult and they have to be treated as variable parameters. However, they cannot be chosen unambiguously. In situations such as this, one is guided by the values of these parameters in the corresponding crystalline phase. By utilising experimental data or the results of more realistic calculations, which are available for the crystalline phases, the tight-binding matrix elements have been obtained for several crystalline phases. They are then used for the amorphous phase. However, in a Bethe lattice calculation, in order to reproduce the top of the valence band at zero energy, the diagonal matrix elements have been normalised. For cases where the necessary information is not available, the familiar $1/d^2$ law used by Harrison (1980) has been invoked to obtain the non-diagonal matrix elements.

The energies of the s , p and s^* type orbitals are denoted by E_s , E_p and E_{s^*} , respectively. The various matrix elements of the Hamiltonian are designated as

$$\begin{aligned}
 U &= \langle s | H | s' \rangle & X &= \langle s | H | p' \rangle & V &= \langle p_x | H | p'_x \rangle \\
 T &= \langle p_x | H | p'_y \rangle & \text{and} & & H &= \langle p | H | s^{*'} \rangle
 \end{aligned}$$

where the orbitals with primes denote the neighbouring sites.

For silicon, the local electronic density of states reveals a smooth and featureless appearance, which compares very well with the photoemission data. The calculated density of states reproduces the two main observed peaks and a forbidden gap of 1.8 eV (see figure 1).

The second and more distant neighbour interaction integrals were obtained by assuming an exponential decay of the first neighbour interaction of the form $V(r) = V_{nn}(a) \exp[-(r-a)/b]$, where $r \geq a$, r being the nearest-neighbour separation; $V_{nn}(a)$ are the nearest-neighbour interactions for separation a and b is an arbitrary constant. The value of b has been fixed by fitting the values of the first and the second neighbour interaction integrals to the above assumed form for a-Si and a-Ge. It gives $b = 0.99 \text{ \AA}$. The values of the used parameters for the various bonds are contained in table 1. For the other details of the CBLM method, we refer the reader to earlier articles (Agrawal and Agrawal 1984, 1987, Agrawal 1980, 1982).

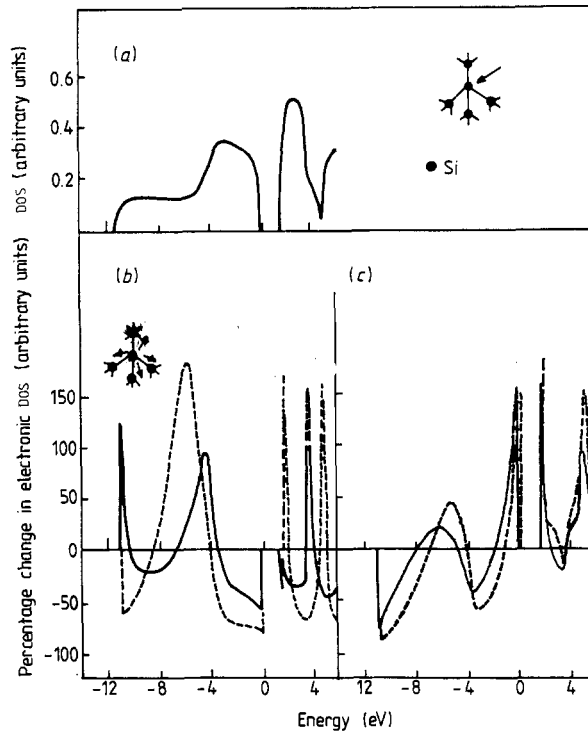


Figure 1. (a) Local electronic density of states (DOS) of amorphous silicon (a-Si). Percentage changes in electronic DOS in a-Si for Si-Si bond length (b) contracted by 10% (—) and 20% (---) and (c) elongated by 10% (—) and 20% (---); A_1 symmetric deformation.

3. Structural defects

3.1. Bond length changes

In an amorphous network an obvious disorder occurs from the distribution of bond lengths between atoms. Here we investigate the changes in the electronic density of states incurred by compressed or stretched Si-Si bonds. The interaction integrals are supposed to follow a $1/d^2$ law (d being the bond length) and the atomic orbital energies are kept unchanged.

The changes in the electronic density of states for the compressed and stretched Si-Si bonds in A_1 symmetry are shown in figure 1. For 10% reduction in bond length (figure 1(b)), the electronic density of states drops at both the band edges of the energy gap, which compensates the enhancements in states in the bulk band region and just at the bottom of the valence band. For the sake of completeness, we reproduce here the bulk density of states for amorphous silicon (a-Si) in figure 1(a). For a 20% decrease in bond length (figure 1(b)), the density not only drops near the top of the valence band but also at the bottom of the valence band. Enhancement in states appears at the conduction band edge.

For stretched bonds (figure 1(c)), the results are quite different. One observes enhancement in the states at both the band edges. These states would behave as tail states in an amorphous network where the stretched bonds would occur throughout the

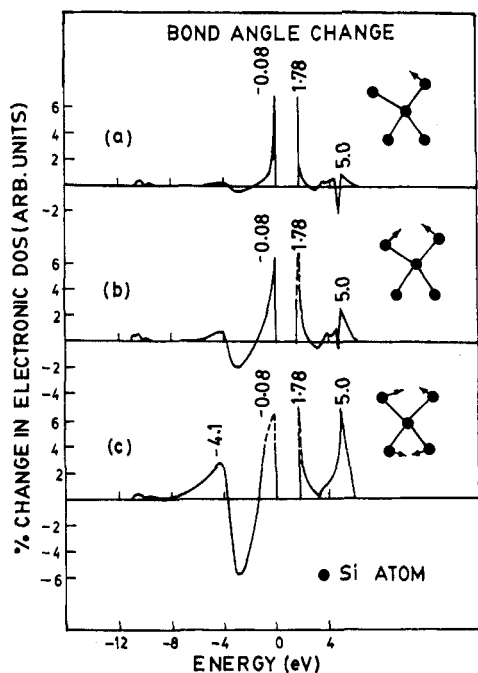


Figure 2. Percentage changes in electronic DOS in a-Si for contraction in (a) one bond angle by 5%, (b) one bond angle by 10% and (c) two bond angles by 10%.

network, in contrast to the presently discussed case where changes in bond lengths of only one single unit have been considered.

3.2. Bond angle changes

Bond angle changes lead to increase in the density of states (DOS) at both the band edges of the fundamental gap (figure 2), which depend on the number and magnitude of bond angle changes. Figure 3 shows the changes in the DOS for distortion at the various tetrahedral interatomic bond angles. The bond angles are changed by different amounts but all lie within 3–10% of the equilibrium value. As an example, in figure 2(c), four of the six bond angles have been changed by 5% and the other two by 10%. The present results are in agreement with those of Joannopoulos (1977) and Singh (1981).

3.3. Dangling bonds

There is current debate (Fedders and Carlsson 1987, 1988, 1989, Pantelides 1986, 1987a, b) as to the atomic structure of the defects leading to the D levels observed (Pankove 1984, Joannopoulos and Lucovsky 1984) in the band gap of a-Si. It has been widely accepted that they originate from dangling bonds involving three-coordinated Si. However, Pantelides has proposed that the gap states may originate from a five-coordinated Si atom involving a 'floating bond'. We confine ourselves here to the electronic structure of the relaxed dangling bonds.

The gap state for an unrelaxed dangling bond of mixed s, p, s* character appears at 0.86 eV (figure 3). This value, which has been measured with respect to the top of the valence band, is quite close to a value obtained by Fedders and Carlsson, who have

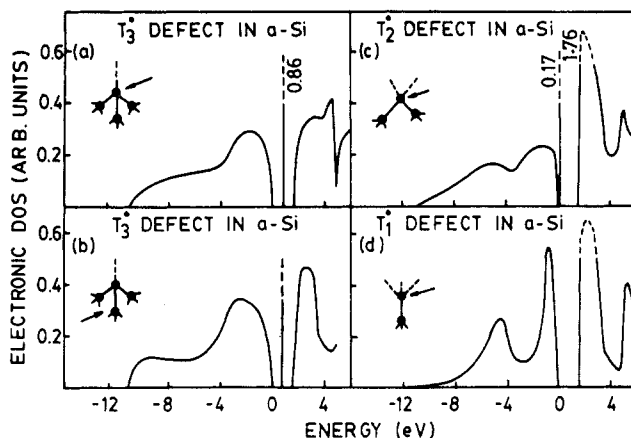


Figure 3. Local electronic DOS in a-Si at (a) T_3^0 defect (single dangling bond), (b) T_3^0 defect at atom neighbouring under-coordinated atom, (c) T_2^0 defect (double dangling bond) and (d) T_1^0 defect (triple dangling bond).

Table 2. Effect of bond length changes on gap states incurred by under coordinated atoms.

Bond length change (%)	T_3^0 (eV)	T_2^0 (eV)
-10	0.79	0.05
-5	0.83	1.69
0	0.86	0.17
+5	0.88	1.76
+10	0.90	0.23
		1.77
		0.29
		1.78

reproduced the energy gap of magnitude 1.7 eV and seen the dangling bond state appearing at 0.7 eV below the conduction band. Also, the present value is very near to the experimental value of 0.8 eV for the measured fundamental gap of 1.8 eV (Street 1985).

Relaxing Si-Si bond lengths by 10% shifts the gap state by only 0.06 eV (see table 2). On the other hand, a relaxation in the bond angles leads to significant changes in the location of the gap states. The shifting has been depicted in table 3. For a contraction of angles by 10%, the state shifts by -0.4 eV, whereas for the enlargement of the bond angles by the same magnitude, we observe a larger shift of 0.7 eV. To sum up, the dangling bond is shifted towards the lower (higher) energy side for the smaller (larger) values of the interatomic bond angles formed at the three-fold coordinated Si atom.

For double (T_2^0) and triple (T_1^0) dangling bonds, the DOS are shown in figures 3(c) and (d), respectively. They reveal gap states appearing at the edges of the fundamental

Table 3. Shifting of dangling bond gap state with changes in the interatomic bond angles.

S. no.	Bond angle change (%)	Location of gap states (eV)
1	-10.0	0.49
2	-5.0	0.65
3	0.0	0.86
4	5.0	1.12
5	10.0	1.55

Table 4. Changes in the location of the gap states caused by the relaxation of Si atoms around vacancy in Si.

S. no.	Change in second neighbour bond length (%)	Location of gap states (eV)
1	10	0.29
		1.06
2	5	0.20
		1.10
3	0	0.11
		1.13
4	-5	0.03
		1.18
5	-10	-0.03
		1.24

gap. For the T_1 defect these localised states enter into the bands. For the relaxed T_3^0 and T_2^0 defects, the states will also enter into the bulk bands.

3.4. Vacancies and divacancies

Irradiation of crystalline silicon introduces defects such as monovacancies, divacancies, multivacancy aggregates, vacancy-impurity pairs and self-interstitials. Of these, the monovacancy (V_1) has been studied most extensively both theoretically and experimentally. It is highly mobile in the lattice.

The occurrence of vacancies in the amorphous phase of Si is not very likely. However, we investigate the defect to check the reliability of the CBLM method. The present calculation has been performed for both the unrelaxed and the symmetrically relaxed vacancy. The DOS for the unrelaxed vacancy reveals two gap states of mixed (s, p) character having A_1 (singlet) and F_2 (triplet) symmetries at 0.11 and 1.13 eV, respectively. For weak second neighbour Si-Si interactions the two split states of a single dangling bond become closer, approaching towards the location of a dangling bond gap state. For a relaxation of the surrounding atoms by +5%, the upper state shifts by about -0.05 (+0.05) eV and the lower state shifts by double this amount, but in the opposite direction. The shift in energy of those levels with relaxation of first neighbouring Si atoms are shown in table 4. Of the four electrons on the surrounding Si atoms, two

occupy the lower non-degenerate A_1 state and two the triply degenerate F_2 state. The vacancy thus undergoes a Jahn–Teller distortion of a tetragonal or trigonal type having lower point group symmetry. These distortions lead to a shifting of the calculated energy levels. On the other hand, in the crystalline phase, the self-consistent calculation of Bernholc (1980) has predicted the two states at -1.1 and 0.76 eV. This large splitting of 1.8 eV will appear for a stronger second neighbour interaction. Gap levels due to a single vacancy in Si have not been accurately determined by experiment. For a detailed discussion of the system, we refer to Lannoo (1984).

In order to see the applicability of the CBLM to more complex systems, we have studied a divacancy, which has been seen to occur in c-Si. Unlike the monovacancy, the divacancy in silicon, like all other associated point defects, has mostly been studied experimentally. Watkins and Corbett (1963) investigated the divacancy in electron-irradiated silicon by electron paramagnetic resonance (EPR) and noted that a divacancy gives rise to three levels in the band gap with four different charge states, V_2^+ , V_2^0 , V_2^- and V_2^{2-} . Photoconductivity measurements (Cheng *et al* 1966, Kalma and Corelli 1968, Young and Corelli 1972) located the V_2^+ charge state 0.26 eV above the valence band edge and V_2^0 and V_2^- 0.54 and 0.39 eV below the conduction band edge, respectively. Qualitatively similar level positions have been given by Kimerling (1977), de Wit *et al* (1976) and Sieverts *et al* (1978), who studied the divacancy by using the electron nuclear double-resonance (ENDOR) technique. Here we investigate the electronic structure of the neutral undistorted divacancy for different separation of the vacancy centres.

The levels of an isolated vacancy having T_d symmetry get split for a divacancy that possesses lower (D_{3d}) symmetry. Gap states of mixed character appear at 0.21 , 0.47 , 1.11 and 1.17 eV. Two of these are doublets, making a total number of six states corresponding to the six dangling bonds of the divacancy. The experimental value for neutral divacancy has not been reported. However, Cheng *et al* (1966), Kalma and Corelli (1968) and Young and Corelli (1972), respectively, have measured the levels at $E_v + 0.26$ eV and $E_c - 0.54$ eV corresponding to one positively charged and one negatively charged state of the divacancy. However, the present results differ in the number and position of the gap states from those calculated by Lindefelt and Liang (1988), who obtained two levels at 0.6 and 1.08 eV by employing a local environment approach in a recursion method. With increased separation between the two component vacancies in a divacancy defect, as expected, the states of a nearest-neighbour divacancy in the middle of the gap shift towards the band edges, for the non-interacting isolated vacancies. Thus for the second neighbour divacancies, gap states appear at -0.07 , 0.22 , 0.78 , 0.99 , 1.16 and 1.76 eV, and for the third neighbour divacancy, states corresponding to the eight interacting dangling bonds appear at 0.04 , 0.15 , 0.89 , 1.1 , 1.18 and 1.41 eV, respectively. Interactions up to third neighbours have been considered in these calculations.

4. Substitutionals and interstitials

We have studied substitutional impurity atoms in a-Si and interstitial atoms in a silicon matrix. The orbital energies of the dopant have been equated to the atomic values and used as the diagonal elements of the Hamiltonian. However, all the E_s and E_p values have been increased by 9.60 and 8.82 eV, respectively. These increases were earlier found necessary to position the upper valence band edge of a-Si at the vacuum level. The values of the nearest-neighbour interaction integrals were obtained from the well

known $1/d^2$ law in which d is the bond length. The atoms are likely to adopt their chemically preferred radius. The bond length d is taken to be the sum of the covalent radii of the two atoms of the bond. These are listed in table 5.

4.1. Substitutional impurities

For substitutional impurities, which include all elements from group II to IV of the periodic table, we have calculated the DOS at the impurity and nearest-neighbour host sites. A perusal of table 5 reveals that elements of groups II and III give rise to acceptor states with T_2 symmetry near the valence band edge. Neither the covalent radii nor the atomic orbital energies of the impurities appear to have a significant influence on the position of the gap states. For small ions like Be and B with low-lying sp^3 hybrid orbitals, there are no states near the band edges of the gap. However, a localised state of character does appear at -10.9 eV for B just below the bottom of the valence band.

For the group IV elements, C and Ge, gap states with A_1 symmetry are found at the conduction band edge in the gap with energies close to 1.7 and 1.78 eV. For Sn with higher s and p atomic orbital energies we find a localised state in the conduction band.

Group V elements lead to donor states with A_1 symmetry, which are close to the conduction band edge. Once again, the effects of impurity size and orbital energy levels appear to be insignificant, except for the N ion, which gives rise to a donor state 0.3 eV below the conduction band. Group V elements other than N lead to localised states just below the valence edge.

The group VI elements, S, Se and Te, lead to A_1 donor states deep into the gap. Oxygen, with a low-lying sp^3 hybrid orbital, gives rise to an A_1 level at the upper valence band edge. In common with the group V elements, localised states are also found below the valence band. The present results are in good qualitative agreement with the self-consistent Green function calculation results of Scheffler *et al* (1984) for crystalline silicon.

4.2. Interstitials

We have calculated the localised DOS for interstitial atoms at symmetric tetrahedral sites at both the impurity and the nearest-neighbour silicon sites. The length of each bond coupling the interstitial atom to the nearest neighbouring atoms is the same and equal to the Si–Si bond length. The gap states are shown in figure 4.

4.2.1. Group II elements. As shown in table 5, valence orbital energies of group II elements like Be, Zn, Mg and Cd are high so that this does not lead to localised states below the valence band of Si. However, they give rise to two states in the fundamental gap: one has A_1 symmetry and is in the middle of the gap; the other of T_2 symmetry is near the conduction band edge. In the case of Zn and Cd, they appear at 0.76 and 1.73 eV and at 0.99 and 1.78 eV, respectively.

4.2.2. Group III elements. Since the orbital energies of the group III atoms are lower than those of group II, the localised impurity states are shifted to lower energy. Consequently, the localised A_1 states occur close to the bottom of the valence band. Gap states are also shifted to lower energy, so that the A_1 state now occurs very near the valence band edge. Interstitial boron is generated in boron-doped crystalline silicon by electron irradiation at cryogenic temperatures (4–20 K). It has been shown to be a $-U$ defect by

Table 5. Gap states due to substitutional and interstitial atoms in a-Si (eV). The covalent radii are also given (Å).

Group	Elements	Covalent radii	Electronegativity	E_s	E_p	E_s^*	$(E_s + 3E_p)/4.0$	Gap states						
								Sub.	Int.	Sub.	Int.			
								T_2	A_1	T_2	A_1	T_2	A_1	T_2
II	Be	0.975	1.81	1.43	4.68	8.05	3.87				0.75	1.54		
	Zn	1.225	2.22	1.20	5.44	6.57	4.38	-0.04			0.76	1.73		
	Mg	1.301	1.32	2.74	5.83	8.03	4.38	-0.06			1.15	1.76		
	Cd	1.405	1.98	1.90	5.44	6.66	4.56	0.04			0.99	1.78		
III	B	0.853	2.28	-2.94	2.18	10.32	0.90				0.12	1.07		
	Ga	1.222	2.42	-1.77	3.92	7.04	2.50	-0.08			0.08	1.59		
	Al	1.23	1.71	-0.51	3.96	7.10	2.84	-0.08			0.33	1.61		
	In	1.405	2.14	-0.52	4.13	7.15	2.97	-0.04			0.27	1.71		
	Tl	1.704	2.25	-0.32	4.21	6.17	3.08	0.12			0.25	1.78		
IV	C	0.771	2.75	-7.92	-0.15	7.38	-2.09		1.76			0.67		
	Si	1.175	2.14	-3.95	2.30	7.27	0.74					1.24		
	Ge	1.225	2.62	-4.78	2.46	6.58	0.65		1.78			1.22		
	Sn	1.405	2.30	-2.90	2.88	7.45	1.44					1.50		
V	N	0.719	3.19	-13.44	-2.65	7.80	-5.35			1.50		0.36		
	P	1.128	2.52	-7.50	0.49	7.87	-1.51			1.73		0.73		
	As	1.223	2.82	-7.73	0.91	8.89	-1.25			1.69		0.85		
	Sb	1.405	2.46	-5.20	1.58	7.35	-0.12			1.72		1.10		
	Bi	1.545	2.34	-4.55	1.85	7.05	0.25			1.68		1.24		
VI	O	0.678	3.65	-19.54	-5.31	3.93	-8.87		0.0		0.16	1.54		
	S	1.127	2.96	-11.20	-1.45	5.17	-3.89			1.06		0.27		
	Se	1.225	3.01	-10.72	-0.71	5.35	-3.21			1.12		0.38		
	Te	1.405	2.62	-7.51	0.23	5.93	-1.71			1.38		0.60		

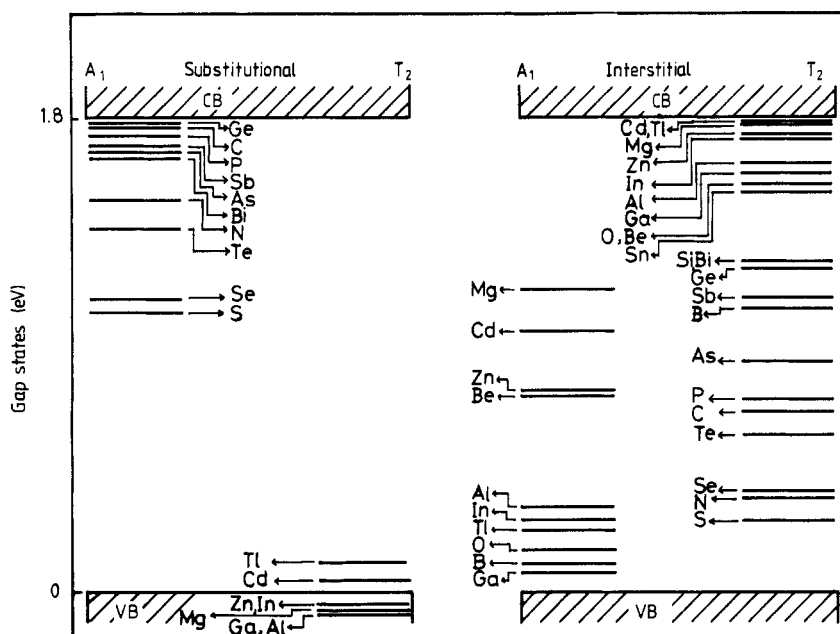


Figure 4. Localised gap states incurred by substitutional and interstitial atoms in a-Si.

electron paramagnetic resonance (EPR) and deep-level transient spectroscopy (DLTS) measurements by Watkins and Troxell (1980a, b) and Harris *et al* (1987). These authors have estimated the location of a single acceptor B state at 0.37 eV and a donor state of B at 0.13 eV below the conduction band edge. They have also suggested non-tetrahedral lattice configurations associated with interstitial B, which are responsible for the two levels. This is the subject of further study.

For an Al interstitial in tetrahedral symmetry, Baraff and Schluter (1984) obtained an A_1 state at 0.2 eV above the valence band edge from a simple-cubic pseudopotential calculation. This is in good agreement with the present value of 0.33 eV. However, their calculated T_2 symmetry state is in the conduction band, in contrast to the present calculation, which locates it 1.61 eV below the conduction band.

4.2.3. Group IV elements. The group IV elements, Ge, C and Sn, which are isovalent to Si, give rise to localised and resonance states of A_1 and T_2 symmetry above the valence band edge and deep into the gap. Thus for Si, defect states appear at -10.9 and 1.24 eV. The former is of s character and A_1 symmetry and the latter p character and T_2 symmetry. The Ge interstitial state is located at 1.22 eV while that of C, whose atomic orbital energies are low, is in the lower half of the gap.

The present result for the Si interstitial is in good agreement with the other theoretical results for crystalline silicon (c-Si) (Sankey and Dow 1983). Bar-Yam and Joannopoulos (1984) have obtained states at -13.0 eV (A_1), -0.5 eV (A_1) and 1.5 eV (T_2) from a pseudopotential density-functional calculation. Similarly, Baraff and Schluter (1984) predicted resonance states of A_1 symmetry near both the edges of the valence band and a gap state of T_2 symmetry near the bottom of the conduction band from a self-consistent Green function calculation using ionic pseudopotentials and the Ceperley–Alder local

potential for exchange and correlation. It should be noted that these self-consistent calculations predict a band gap in Si that is smaller than the experimental value.

The elements of group V also lead to a localised state of T_2 symmetry in the gap and a second near the lower valence band as shown in table 5. The location of the gap state shifts to higher energy as the covalent radius increases or the atomic orbital energies of an interstitial are enhanced. Thus for N, a gap state is produced at 0.36 eV; for Bi, at 1.24 eV.

For group VI interstitials, a single gap state of T_2 symmetry is found in the lower part of the gap. The exception being O, for which two localised states of A_1 and T_2 symmetry are predicted. These are an A_1 state at 0.16 eV and T_2 state at 1.54 eV. The present results are in good agreement with those from a self-consistent Green function calculation reported by Scheffler *et al* (1984) for S in crystalline silicon. The present observed chemical trends of the occurrence of gap states induced by interstitials belonging to different groups of the periodic table is in agreement with Sankey and Dow (1983).

5. Conclusions

A cluster Bethe lattice method has been shown to be capable of providing reliable qualitative and semiquantitative information about the states introduced by impurities and point defects and their complexes in amorphous material like a-Si. Structural disorder such as bond length and bond angle variations give rise to shallow states very near the upper edge of the valence band and lower edge of the conduction band. The effect of the bond angle disorder dominates and has been shown to be quite significant. This is also true for relaxed dangling bonds. The position of deep levels associated with dangling bonds or vacancies appear to be specially sensitive to changes in nearest-neighbour bond angles.

Elements from groups II and III substituted in silicon give rise to shallow T_2 states near the valence band edge whereas group V elements, in general, lead to gap states of A_1 symmetry near the conduction band edge. Group VI elements on the other hand give rise to A_1 states deep in the gap, except for oxygen, which produces a state at the valence band upper edge.

At interstitial sites with tetrahedral symmetry, group II and III elements are predicted to lead to two states in the band gap: one of A_1 symmetry, the other T_2 . For group II interstitials, they are both deep in the gap; for group III elements, on the other hand, while the T_2 state is deep in the gap, the A_1 state occurs near the valence band upper edge. Group IV interstitials produce T_2 states in the upper half of the gap, except for the C atom, which generates a state in the lower half of the gap. Group V elements lead to deep states of T_2 symmetry throughout the band gap depending on the covalent radius, while the T_2 states of group VI interstitials are in the lower half of the band gap, except for oxygen, which generates two gap states, one of A_1 symmetry near the valence band edge, the other of T_2 symmetry near the conduction band edge. In general, within any group, an increase in energies for the T_2 gap states is observed with increase in the covalent radius except for relatively small atoms such as B, C and O.

Acknowledgments

The present work was supported by the Department of Science and Technology, New Delhi, and by University Grants Commission, New Delhi.

References

- Agrawal B K 1980 *Phys. Rev. B* **22** 6294
— 1982 *Phys. Rev. B* **26** 5972
Agrawal B K and Agrawal S 1984 *Phys. Rev. B* **29** 6870
— 1987 *Phys. Rev. B* **36** 2799
Baraff G A and Schluter M 1984 *Phys. Rev. B* **30** 3460
Bar-Yam Y and Joannopoulos J D 1984 *Phys. Rev. B* **30** 1844
Bernholc J 1980 *Phys. Rev. B* **21** 3545
Cheng L J, Corelli J C, Corbett J W and Watkins G D 1966 *Phys. Rev.* **152** 761
de Wit J G, Sieverts E G and Ammerlaan C A J 1976 *Phys. Rev. B* **14** 3494
Fedders P A and Carlsson A E 1987 *Phys. Rev. Lett.* **58** 1156
— 1988 *Phys. Rev. B* **37** 8506
— 1989 *Phys. Rev. B* **39** 1134
Harris R D, Newton J L and Watkins G D 1987 *Phys. Rev. B* **36** 1094
Harrison W A 1980 *Electronic Structure and the Properties of Solids* (San Francisco: Freeman)
Joannopoulos J D 1977 *Phys. Rev. B* **16** 2764
Joannopoulos J D and Lucovsky G 1984 *The Physics of Hydrogenated Amorphous Silicon II* (Berlin: Springer)
Kalma A H and Corelli J C 1968 *Phys. Rev.* **173** 734
Kimerling L C 1977 *Radiation Effects in Semiconductors 1976 (Inst. Phys. Conf. Ser. 31)* ed N B Urli and J W Corbett (Bristol: Institute of Physics) p 221
Lannoo M 1984 *J. Phys. C: Solid State Phys.* **17** 3137
Lindelfelt U and Liang W Y 1988 *Phys. Rev. B* **38** 4107
Pankove J I 1984 *Hydrogenated Amorphous Silicon, Semiconductors and Semimetals* vol 21 (New York: Academic)
Pantelides S T 1986 *Phys. Rev. Lett.* **57** 2979
— 1987a *Phys. Rev. Lett.* **58** 1344
— 1987b *Phys. Rev. B* **36** 3479
Robertson J 1983 *Phys. Rev. B* **28** 4658
Sankey O F and Dow J D 1983 *Phys. Rev. B* **27** 7641
Scheffler M, Beeler F, Jepson O, Gunnarsson O, Anderson O K and Bachelet G 1984 *Proc. 13th Int. Conf. on Defects in Semiconductors* ed L C Kimerling and J M Parsey Jr (New York: Metallurgical Society of AIME) p 45
Sieverts E G, Muller S H and Ammerlaan C A J 1978 *Phys. Rev. B* **18** 6834
Singh J 1981 *Phys. Rev. B* **23** 4156
Street R A 1982 *Phys. Rev. Lett.* **49** 1187
— 1985 *J. Non-Cryst. Solids* **77/78** 1
Vogl P, Hjalmarson H P and Dow J D 1983 *J. Phys. Chem. Solids* **44** 365
Watkins G D and Corbett J W 1963 *Phys. Rev.* **138** A543
Watkins G D and Troxell J R 1980a *Phys. Rev. Lett.* **44** 593
— 1980b *Phys. Rev. B* **22** 921
Young R C and Corelli J C 1972 *Phys. Rev. B* **5** 1455